Oriented Nanomaterial Air Bridges Formed from Suspended Polymer-Composite Nanofibers

Santosh Pabba, Anton N. Sidorov, Scott M. Berry, Mehdi M. Yazdanpanah, Robert S. Keynton, Gamini U. Sumanasekera, and Robert W. Cohn*

ElectroOptics Research Institute & Nanotechnology Center, University of Louisville, Louisville, Kentucky 40292

ARTICLE

ABSTRACT In a two-step method, carbon nanotubes, inorganic nanowires, or graphene sheets are connected between two anchor points to form nanomaterial air bridges. First, a recently developed method of forming directionally oriented polymer nanofibers by hand-application is used to form suspended composite polymer–nanomaterial fibers. Then, the polymer is sacrificed by thermally induced depolymerization and vaporization, leaving air bridges of the various materials. Composite fibers and bundles of nanotubes as thin as 10 nm that span 1 μm gaps have been formed by this method. Comparable bridges are observed by electrospinning solutions of the same nanomaterial–polymer composites onto micrometer-scale corrugated surfaces. This method for assembling nanomaterial air-bridges provides a convenient way to suspend nanomaterials for mechanical and other property determinations, and for subsequent device fabrication built up from the suspended nanosubstrates.

KEYWORDS: nanofabrication · nanostructures · polymer composites · nanomaterials · nanotubes · nanowires · graphene

Many recent nanomaterial device proposals and experimental studies call for the nanomaterial to be suspended as a two-point beam, or "air bridge". This three-dimensional geometry simultaneously creates a nanomechanical element and isolates the element from various substrate effects (except at the supports), *e.g.*, surface adhesion and strain forces, substrate temperature, reduced surface area in contact with the atmosphere, substrate conductivity, and parasitic capacitance. Not only are bridges accessible along the length of such structures, but near-field probing, manipulation, and actuation of suspended nanostructures have provided[1–3] and will continue to provide interesting physical properties and device possibilities.

The typical approaches for fabricating air bridges either (1) disperse nanomaterials in solvents, followed by mapping, lithographic patterning, and undercutting,[1] or (2) selectively grow nanomaterials in high-temperature reactors.[4] The first approach is laborious, and the second requires that an appropriate growth recipe exist for the material of choice.

Previously we, and recently others, showed that suspended nanofibers, as small as 50 nm diameter, are formed by *hand brushing* of solutions of polymer in volatile solvent onto micrometer-scale corrugated surfaces.[5,6] Figure 1A–C illustrates the method. Here we show that this single-step method can be extended to suspending a variety of nanomaterials by similarly forming fibers from solutions of nanomaterials and polymer. The additional step is illustrated in Figure 1D, where the suspended nanomaterial-composite fiber is thermally decomposed to leave an air bridge of the nanomaterial.

Of course, the decomposition step could also be applied to nanofibers formed by processes other than brushing. For instance, Figure 2A shows a composite fiber of multiwall carbon nanotubes (MWNTs) in poly(methyl methacrylate) (PMMA, 996 000 g/mol, Sigma-Aldrich) that has been electrospun onto the tops of micrometer diameter pillars from a chlorobenzene solution containing 1 wt % MWNTs and 4 wt % PMMA. The solution also contains less than 1 wt % of nanotube functionalization and residuals (which are analyzed by TGA, EDS, and Raman as described below.) The nanotube functionalization is an adsorbed organic (trade name Kentera, Zyvex Corp., Richardson, TX) that consists of an alkane group connected to a phenyl end group that adsorbs to the nanotube and an end group that enhances the solubility of the nanotubes in chlorobenzene.[7] The functionalized nanotubes and PMMA are both easily dispersed in chlorobenzene, leading to a well-mixed nanotube–PMMA solution. The electrospun fiber shown in Figure 2A is then placed on a preheated hotplate in air at 450 °C (*i.e.*, the sample is heated rapidly;

*Address correspondence to rwcohn@louisville.edu.

Received for review May 29, 2007 and accepted July 25, 2007.

Published online August 14, 2007.
10.1021/nn700047n CCC: $37.00

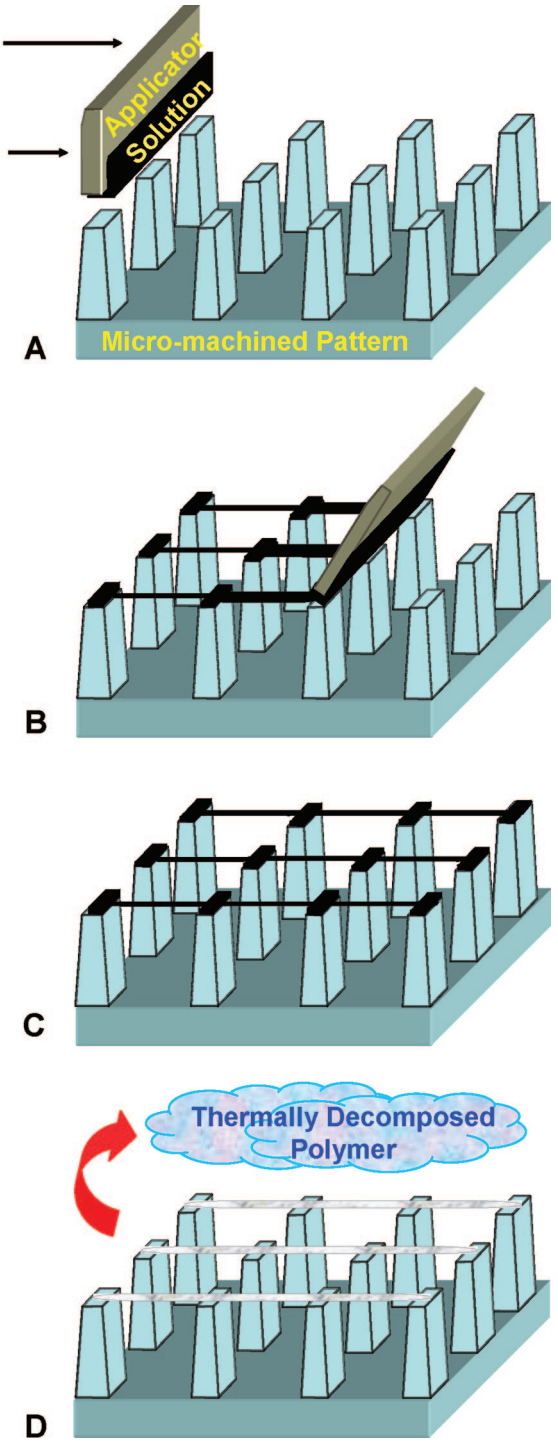

Figure 1. Nanomaterial air bridge fabrication technique. (A) The composite solution on the applicator is (A–B) brushed across the array. The solution wets to the pillars and forms liquid threads between them. The threads thin as they dry (C) until they solidify, leaving suspended composite fibers. (D) The polymer in the fibers is removed by thermal decomposition, leaving air bridges of the nanomaterial.

if instead the sample is heated gradually, the bridges usually sag and fall onto the base of the pillars). The temperature is maintained for 1 h to ensure thorough removal of the polymer. The MWNTs that remain after decomposition form the bridges shown in Figure 2B.

The tapered shape of the nanotube bridge is probably due to capillary thinning of the melted PMMA fiber prior to decomposition, while the broad spreading of the nanotubes on the top of the pillars is probably due to rapid wetting of melted PMMA prior to decomposition. Also note that the bridge shown in Figure 2B is across different pillars than that shown in Figure 2A. In fact, the portion of polymer viewed under the scanning electron microscope (SEM) in Figure 2A did not completely decompose. Apparently the electron beam, which normally scissions the polymer chains when used for electron beam lithography, is also causing the polymer to bond to the nanotubes. The region shown in Figure 2B was not imaged under the SEM prior to decomposition.

If the fibers are formed using the brush-on method (Figure 1A–C), the fibers can be well oriented in the direction of brushing (sometimes with smaller fibers found in the cross direction.) Also, the fibers can be suspended either from the tops of the pillars or from the sidewalls of the pillars. Figure 3A shows sidewall-supported MWNT–PMMA composite fibers formed by brush-on. These were formed by applying a thin bead of solution from a pipet to the edge of an applicator (*e.g.*, a microscope coverslip, flexible plastic sheet, or copper wire) and manually brushing it across the corrugated substrate at a velocity of around 15–35 mm/s. The solution concentration used was 15 wt % PMMA and 0.85 wt % MWNT in chlorobenzene, which results in a solution thin enough that it can strongly wet the pillars and sidewalls. Thick liquid bridges initially form between adjacent sidewalls and then thin due to capillary forces, finally reaching a stable diameter after

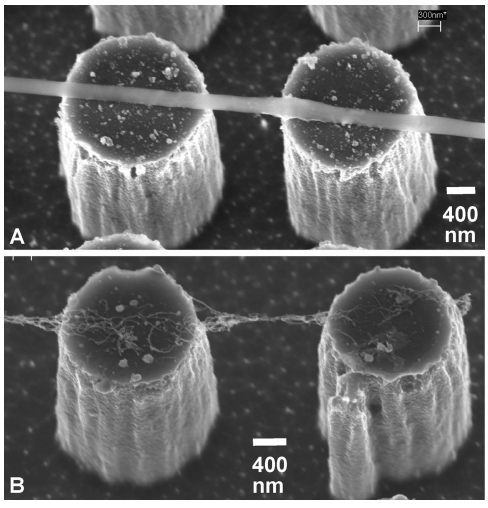

Figure 2. Suspension of MWNTs by sacrificial decomposition of a suspended PMMA–MWNT fiber. (A) An air bridge of the composite fiber and (B) the resulting MWNT air bridge following thermal decomposition of the PMMA in the composite fiber. For electrospinning, the solution was pumped at 0.6 mL/h to a needle 5 cm long × 0.7 mm inner diameter, with 13 kV applied between the needle and pillar array at a separation of 5 cm. The sidewall roughness and particulates on the pillars are due to the conditions used during the plasma etching of this (n-type, 4 Ω-cm) silicon substrate.

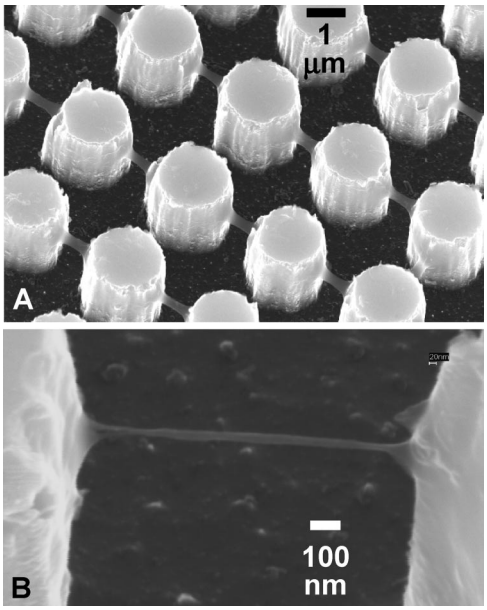

Figure 3. Suspended PMMA–MWNT composite fibers made by hand-brushing. (A) An array of fibers and (B) an isolated 20–30 nm diameter fiber which appears to result from a reduced quantity of solution being applied in this region of the pillar array.

enough of the solvent evaporates.[6,8,9] Increased solution concentrations (up to 40 wt % PMMA in this study) lead to the formation of thicker fibers that are attached closer to the top surface.

Figure 3B shows an isolated fiber from the brush-on experiment processed similarly to the one shown in Figure 3A. This fiber varies between 20 and 30 nm diameter along its length, which is about half the diameter of our previously reported smallest fiber.[6] The nanotubes appear to provide additional reinforcement against the fibers breaking during the process of capillary thinning and fiber solidification. Certainly, we frequently observe that fibers of pure PMMA break (due to melting or decomposition) under the same SEM imaging conditions as used for either image in Figure 3. It should be noted that the SEM images (which are taken without any conductive coating) show only slight charging. Apparently the nanotubes are bridging the pillars, providing a discharge path.

A new sample was prepared by hand brush-on under the same conditions as in Figure 3 (including the same solution and the same substrate, which is cleaned of all organics prior to reuse). The suspended structures shown in Figure 4A,B result after thermal decomposition of the composite fibers at 540 °C. (This same temperature is also used for decomposition of all hand-brushed-on fibers reported below.) In Figure 4A, loose bundles of suspended MWNTs are connected between pillars both in the brushing direction (from upper left to lower right in the image) and orthogonal to the brushing direction. The bundles also show a somewhat tapered appearance, with the minimum diameter midway between the supports. A close-up of one of these bundles is shown in Figure 4B. It has an appearance that reminds one of the children's string art figure called "Jacob's ladder". The nanotubes appear to be roughly aligned between the supports, as a result of the brushing and fiber thinning (which can occur both during brush-on and as the polymer melts.)

Another sample was made by hand brush-on onto the same substrate, this time using a solution of Kentera-functionalized single-wall carbon nanotubes (SWNTs, 0.08 wt %) and PMMA (25 wt %) in chlorobenzene. Figure 4C shows that the resulting array of SWNTs is aligned in the direction of brushing. Figure 4D shows a close-up of one bridge from the array that is ~10 nm in diameter. The SEM cannot resolve whether the bridge consists of a bundle of well-aligned SWNTs or

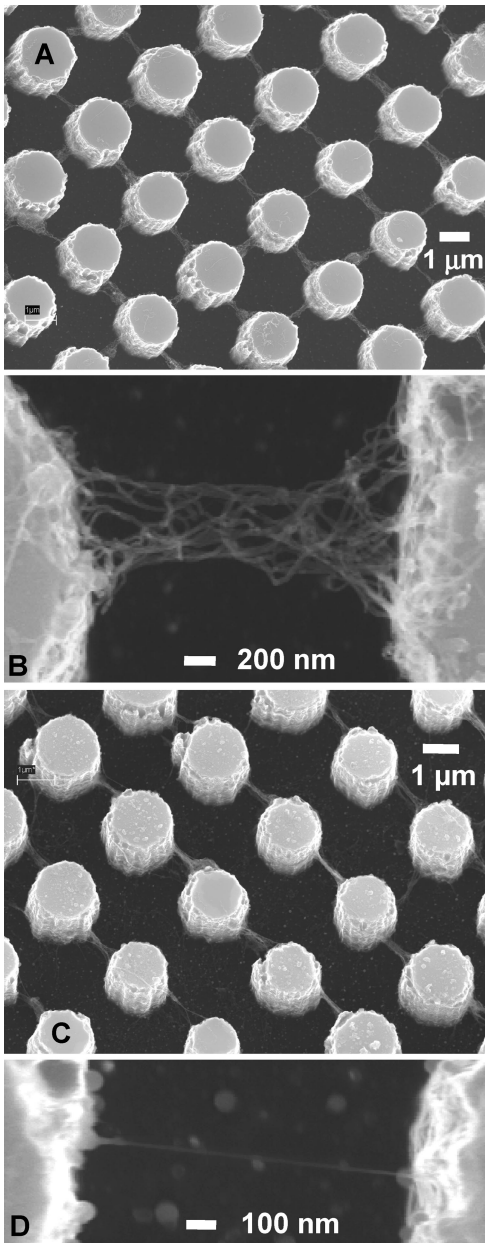

Figure 4. Nanotube air bridges following decomposition of (A,B) MWNT–PMMA and (C,D) SWNT–PMMA fibers.

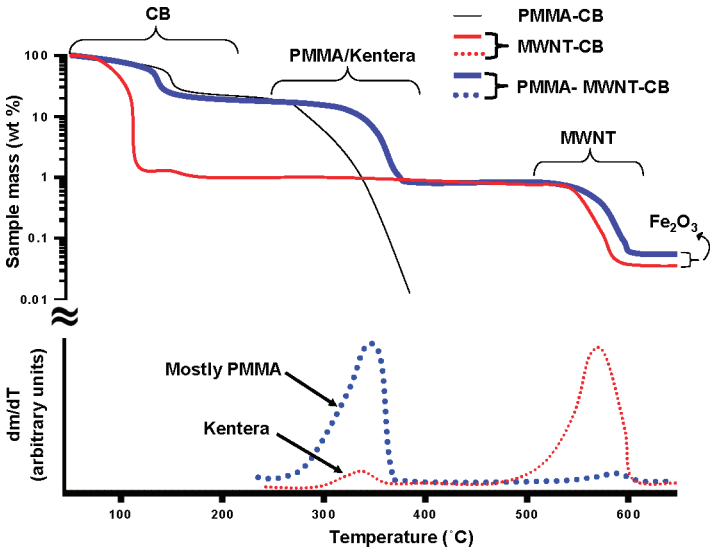

Figure 5. Thermogravimetric analysis of solutions of PMMA and functionalized MWNTs in chlorobenzene (CB). All measurements are performed in air at a heating rate of 5 °C/min. The two dotted lines are derivatives with respect to temperature (d*m*/d*T*) of the corresponding sample mass curves. The derivative curves are plotted on a linear scale. The braces indicate the extent of the peak of each species as determined from derivative curves. All the curves have been smoothed substantially to aid in discussion.

contains other residuals. So far, transmission electron microscopy studies to answer this question have not been successful. Thermogravimetric analysis (TGA), reported below, shows that most residues are removed, but it cannot reliably measure fractional weight changes much below 0.1 wt %. Even without a complete knowledge of the nanomaterial purity, we do consider the ability to form 10 nm suspended nanotube fibers, starting with only hand application of the composite polymer fibers, to be quite remarkable.

TGA of solutions (from 50 to 280 mg) in air was used to identify the decomposition temperatures and residuals. Figure 5 reports on the solution of 15 wt % PMMA and functionalized 0.85 wt % MWNTs in chlorobenzene (thick line), together with reference curves for 15 wt % PMMA in chlorobenzene (thin line) and the Kentera-functionalized 1 wt % MWNTs in chlorobenze (medium line). The Kentera and PMMA peaks (thicker dotted line and medium dotted line, respectively) lie on top of each other. The tails of the PMMA and MWNT barely overlap at 450 °C.

Raman spectroscopy (1.7 mW at 632.8 nm) of samples spun onto a planar SiO_2 substrate further support the composition analyses. (Plots of the Raman spectra of these samples are presented in the Supporting Information.) The removal of Kentera and PMMA changes the intensity ratio of nanotube D (disordered at ~1330 cm^{-1}) to G (ordered at ~1590 cm^{-1}) bands. The appearance of the disorder peak at ~1330 cm^{-1} is known to be associated with a decrease in symmetry of the sp^2 structure due to nanotube defects, including the presence of functionalized groups.[10] The change is most evident when SWNT solutions are used. The ratio of D/G intensities (specifically, the integrated area of the intensity peaks) changes from 0.0715 to 0.0292 after heating of the SWNT–chlorobenzene sample, and for the SWNT–PMMA–chlorobenzene sample the ratio changes from 0.0525 to 0.0099 after heating. For the MWNT–chlorobenzene sample, the ratio of D/G, rather than decreasing (as with the SWNTs), increases from 0.4638 to 0.7107 after heating, and that for the MWNT–PMMA–chlorobenzene sample increases from 0.4357 to 0.6623. The reason for the increase in disorder of MWNTs after heat treatment is not clear without further study. However, we do note that the disorder is much larger than for SWNTs, and the relative change in D/G is much less, as might be expected for a material with less accessible surface area.[11] Also, compared to the changes in SWNTs, the overall changes before and after heat treatment are much less for MWNTs. Also note that both functionalized SWNT and MWNT samples (whether dispersed in PMMA or not) show a peak for Kentera at ~2190 cm^{-1} that completely disappears after the sample is heated to 540 °C.

Additional composition information is available from these TGA and Raman measurements. A very small residue of reddish-brown oxidized iron is found after complete decomposition of the functionalized MWNTs in chlorobenzene. TGA shows that the mass of all residues remaining above 650 °C totals only 5% of the weight of pure (*i.e.*, Kentera-free) MWNTs. Since electron-energy dispersive spectroscopy (EDS) of the residue shows only oxygen and iron, we believe that residual iron catalyst from the growth of the nanotubes was likely present in the MWNT–chlorobenzene solution. Raman spectroscopy of this residue confirms it to be Fe_2O_3, and peaks from other materials were not evident in the spectra. Also, the Kentera peak in the TGA accounts for only 10% of the weight of the pure MWNT. This is close to the percentage of Kentera reported in the material data safety sheet for the functionalized nanotube–solvent solution. In summary, the mass fraction of MWNT:Kentera:Fe_2O_3 is 1:0.1:0.05. TGA of the SWNTs shows similar responses (though noisier due to lower fractions of SWNT), giving a ratio of 1:0.8:0.1 in SWNT:Kentera:Fe_2O_3.

The brush-on method also can be used to form air bridges from other nanomaterials. We present examples of suspending GaAsP nanowires (grown by a laser ablation technique[12]) and graphene sheets (made by exfoliation of powdered, highly ordered pyrolytic graphite (HOPG)). These materials are mixed at ~0.03 wt % GaAsP and ~0.3 wt % HOPG into separate 18 wt % solutions of PMMA in chlorobenzene. The GaAsP suspension was sonicated for 20 min, while the HOPG solution was ultrasonicated for 5 h to promote exfoliation of graphene sheets. No functionalization is used to dis-

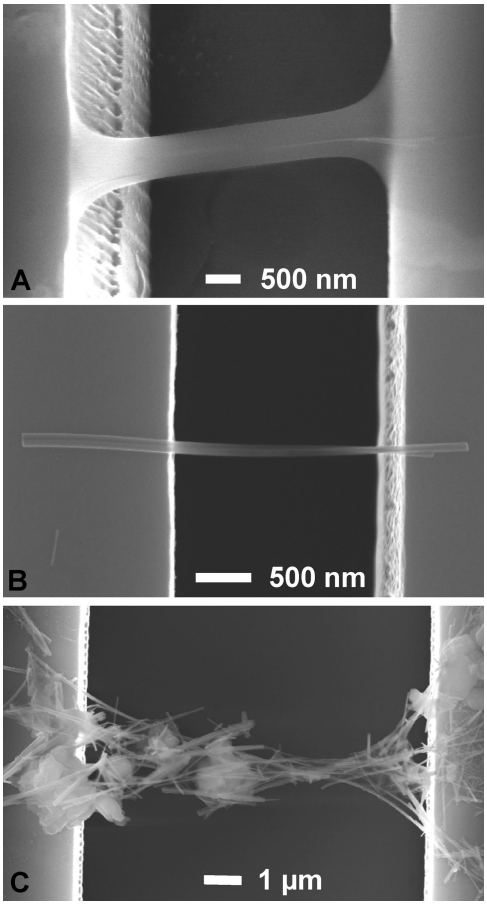

Figure 6. Suspended bridges of (A) PMMA–GaAsP fiber (with a nanowire somewhat visible in PMMA) and two GaAsP nanowire bridges after thermal decomposition, resulting in (B) two nanowires that are closely bundled and (C) a network of nanowires plus residual ebeam-carbonized/cross-linked PMMA.

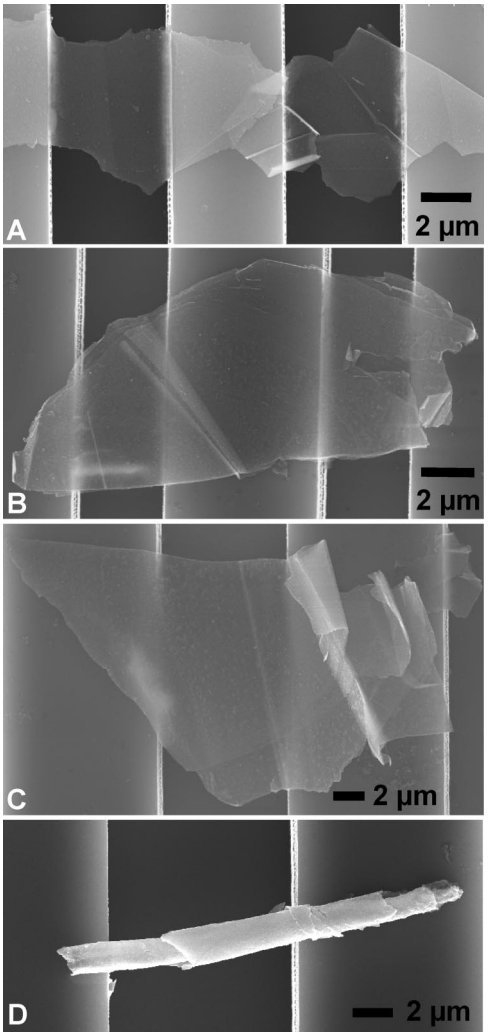

Figure 7. Suspended graphene formed by fiber brush-on and thermal decomposition. Step edges and curling of delaminated sheets are evident in each SEM image, with the degree of curling increasing from (A) to (D).

perse the nanomaterials, so they rapidly settle. As a result, the solution applied to the applicator has less than 0.01 wt % nanowires and 0.1% graphene. Suspended structures produced by brush-on of these suspensions are shown in Figures 6 and 7.

Figure 6A shows a composite fiber in which at least one GaAsP nanowire is visible. Figure 6B shows a bundle of two nanowires formed after thermal decomposition of PMMA. In Figure 6C, for a fiber that was imaged by SEM prior to decomposition, two features are evident. First, the bridge is tapered in a similar way as the nanotube bridges in Figure 4, which again suggests that the shape is caused by surface wetting and capillary thinning as the polymer melts, prior to decomposition. Second, residues of the PMMA are present, as a result of having imaged this fiber in the SEM prior to thermal decomposition.

Figure 7 shows an assortment of graphene bridges. These sheets are rather thick (typically around 15 nm or 44 atomic monolayers thick, as determined by atomic force microscopy) due to limitations in the exfoliation process.[13] However, thinner steps between layers are also evident. Also, the samples show different degrees of curling and delamination from the edges, even rolling up into an isolated tube in Figure 7D.

A brief comment on the reliability and controllability of making nanomaterial air bridges is in order. While no detailed yield studies have been performed, in our casual observations of SEM images of 30 nanotube brush-on experiments with MWNT solution, pillar arrays, and processing conditions similar to those used in Figure 3A, we observed a local area of sometimes as many as 30 nanotube air bridges without a single missing bridge. For much larger areas (300 pillars), in the worst case, we found as many as 75% of the bridges missing (starting from 95% nanofiber composite bridges.) However, for this worst-case sample, most of the nanocomposite fiber bridges had diameters between 50 and 150 nm (as compared to diameters around 200–400 nm for most typical samples). For the graphene and GaAsP nanowires, we have much less material available, which has limited us to only a few experiments with much lower concentrations compared

to the concentrations of available nanotube solutions. Even with these low concentrations, we frequently found three or four consecutive bridges (similar to Figure 6B) for the GaAsP nanowires formed from a single fiber, and two consecutive bridges for graphene (similar to Figure 7A).

In developing control of the process, two conditions need to be kept in mind. These are that the polymer fibers must span the supports and that the nanomaterials in the polymer also must span the supports. A further condition (as pointed out above) is that the polymer must be heated rapidly enough so that it decomposes before it begins to fall apart due to reflow. Related to these conditions, as the nanomaterial concentration decreases or the polymer fiber diameter decreases, the probability of a nanomaterial spanning a gap decreases. Also, it is not required that a single nanowire or nanotube span the entire gap, but clusters and bundles of shorter length nanomaterials promoted by wetting and adhesion (*e.g.*, suggested by Figures 4B and 6C) can span the gap. The two above conditions also are related to controlling the dimensions of the resulting air bridges. That is, the diameter of the initial nanocomposite polymer fiber[8,9] and its concentration of nanomaterials will strongly affect the resulting diameter after thermal decomposition of the polymer. Furthermore, densification due to wetting and adhesion would need to be considered.

In summary, micro- and nanoscale polymer fiber bridges reinforced with nanostructures such as nanotubes, nanowires, and graphite sheets were successfully drawn using manual brush-on and electrospinning techniques. Composition analysis seems to suggest near-complete removal of residues. Some alternatives to the processes reported here that can be considered are the use of lower temperature decomposition polymers or conditions that favor nanotube decomposition at higher temperatures (*e.g.*, decomposition under an atmosphere of nitrogen.) We also had attempted solvent dissolution of the polymers with limited success.[14] While suspended fibers could be produced, organic residues, most likely Kentera, were present and in fact appeared to be essential for maintaining the structural integrity of the air bridges. The process of brush-on followed by thermal decomposition provides a new tool for fabricating test structures for the evaluation and characterization of suspended nanomaterials, which supports the development of new nanoelectronic devices and nanoelectromechanical systems.

Acknowledgment. Mark M. Crain (University of Louisville) fabricated the pillar arrays, and Romaneh Jalilian (University of Louisville) synthesized the GaAsP nanowires. This study was partially supported by National Science Foundation grant ECS-0506941 and National Aeronautics and Space Administration cooperative agreement NCC5-571.

Supporting Information Available: Raman spectra of SWNT–Kentera, SWNT–Kentera–PMMA, MWNT–Kentera, and MWNT–Kentera–PMMA before and after thermal decomposition. This material is available free of charge *via* the Internet at http://pubs.acs.org.

REFERENCES AND NOTES

1. Bunch, J. S.; Van der zande, A. M.; Verbridge, S. S.; Frank, I. W.; Tanenbaum, D. M.; Parpia, J. M.; Craighead, H. G.; McEuen, P. L. Electromechanical Resonators from Graphene Sheets. *Science* **2007**, *315*, 490–493.
2. Mann, D.; Pop, E.; Cao, J.; Wang, Q.; Goodson, K.; Dai, H. J. Thermally and Molecularly Stimulated Relaxation of Hot Phonons in Suspended Carbon Nanotubes. *J. Phys. Chem. B* **2006**, *110*, 1502–1505.
3. Tombler, T. W.; Zhou, C.; Alexseyev, L.; Kong, J.; Dai, H.; Liu, L.; Jayanthi, C. S.; Tang, M.; Wu, S. Y. Reversible Electromechanical Characteristics of Carbon Nanotubes under Local Probe Manipulation. *Nature* **2000**, *405*, 769–772.
4. Cao, J.; Wang, Q.; Dai, H. Electron Transport in Very Clean, as-grown Suspended Carbon Nanotubes. *Nat. Mater.* **2005**, *4*, 745–749.
5. Guan, J.; Yu, B.; Lee, L. J. Forming Highly Ordered Arrays of Functionalized Polymer Nanowires by Dewetting on Micropillars. *Adv. Mater.* **2007**, *19*, 1212–1217.
6. Harfenist, S. A.; Cambron, S. D.; Nelson, E. W.; Berry, S. M.; Isham, A. W.; Crain, M. M.; Walsh, K. M.; Keynton, R. S.; Cohn, R. W. Direct Drawing of Suspended Filamentary Micro- and Nanostructures from Liquid Polymers. *Nano Lett.* **2004**, *4*, 1931–1937.
7. Rutkofsky, M.; Folaron, R. Zyvex's NanoSolve Technology: An Applications Overview; Zyvex Application Note 9714; Zyvex Corp.: Richardson, TX, 2006.
8. Tripathi, A.; Whittingstall, P.; McKinley, G. H. Using Filament Stretching Rheometry to Predict Strand Formation and 'Processability' in Adhesives and Other Non-Newtonian Fluids. *Rheol. Acta* **2000**, *39*, 321–337.
9. Berry, S. M.; Harfenist, S. A.; Keynton, R. S.; Cohn, R. W. Characterization of Micromanipulator-Controlled Dry Spinning of Micro- and Sub-microscale Polymer Fibers. *J. Micromech. Microeng.* **2006**, *16*, 1825–1832.
10. Utegulov, Z. N.; Mast, D. B.; He, P.; Shi, D.; Gilland, R. F. Functionalization of Single-walled Carbon Nanotubes Using Isotropic Plasma Treatment: Resonant Raman Spectroscopy Study. *J. Appl. Phys.* **2005**, *97*, 104324.
11. Yu, A.; Hu, H.; Bekyarova, E.; Itkis, M. E.; Gao, J.; Zhao, B.; Haddon, R. C. Incorporation of Highly Dispersed Single-Walled Carbon Nanotubes in a Polyimide Matrix. *Compos. Sci. Technol.* **2006**, *66*, 1190–1197.
12. Gudiksen, M. S.; Lauhon, L. J.; Wang, J.; Smith, D. C.; Lieber, C. M. Growth of Nanowire Superlattice Structures for Nanoscale Photonics and Electronics. *Nature* **2002**, *415*, 617–620.
13. Stankovich, S.; Dikin, D. A.; Dommett, G. H. B.; Kohlhaas, K. M.; Zimney, E. J.; Stach, E. A.; Piner, R.D.; Nguyen, S.T.; Ruoff, R.S. Graphene-based Composite Materials. *Nature* **2006**, *442*, 282–286.
14. Pabba, S.; Berry, S. M.; Yazdanpanah, M. M.; Keynton, R. S.; Cohn, R. W. Nanotube Suspension Bridges Directly Fabricated from Nanotube-Polymer Suspensions by Manual Brushing. *IEEE-Nano: Sixth IEEE Conf. Nanotechnol.* **2006**, *2*, 565–569.